Charge and spin order in the perovskite CaFe_{0.5}Mn_{0.5}O_{3}: Charge disproportionation behavior of randomly arranged Fe^{4+}

Yoshiteru Hosaka, Noriya Ichikawa, Takashi Saito, J. Paul Attfield, and Yuichi Shimakawa

Phys. Rev. B **94**, 104429 — Published 26 September 2016

DOI: 10.1103/PhysRevB.94.104429

Charge and spin order in the perovskite $CaFe_{0.5}Mn_{0.5}O_3$: Charge disproportionation behavior of randomly arranged Fe^{4+}

Yoshiteru Hosaka[1], Noriya Ichikawa[1], Takashi Saito[1], J. Paul Attfield[2], Yuichi Shimakawa[1]

[1] Institute for Chemical Research, Kyoto University, Uji, Kyoto 611-0011, Japan
[2] Centre for Science at Extreme Conditions and School of Chemistry, University of Edinburgh, Mayfield Road, Edinburgh EH9 3JZ, United Kingdom

PACS codes 75.47.Lx, 75.50.Gg, 71.45.Lr

Abstract

B-site-disordered perovskite $CaFe_{0.5}Mn_{0.5}O_3$ with unusually high valence Fe^{4+} was synthesized using a high-pressure technique. Fe^{4+} randomly distributed at the half of the *B* sites shows charge disproportionation to Fe^{3+} and Fe^{5+}. The spins of Fe^{3+}, Fe^{5+} and Mn^{4+} order below 90 K. Analysis of low-temperature neutron powder diffraction data revealed a G-type antiferromagnetic structure—where all the nearest neighboring spins of Fe^{3+}, Fe^{5+}, and Mn^{4+} couple antiparallel— and the small ordered moment of 0.58 μ_B reveals local charge ordering that gives rise to predominant Fe^{3+}-O-Fe^{5+} antiferromagnetic arrangements. Despite the identical chemical compositions of $CaFe_{0.5}Mn_{0.5}O_3$ and Ca_2FeMnO_6, the magnetic structure of the present $CaFe_{0.5}Mn_{0.5}O_3$ is very different from the noncollinear one of layered *B*-site -ordered Ca_2FeMnO_6.

Introduction

At low temperature some perovskite structure oxides with the unusually high valence Fe^{4+} show characteristic charge behaviors relieving the instability of the high valence state. The simple perovskite $CaFeO_3$ and the *A*-site-ordered perovskite $CaCu_3Fe_4O_{12}$ are examples of such oxides, and they show a charge disproportionation (CD) transition in which Fe^{4+} changes to Fe^{3+} and Fe^{5+} ($2Fe^{4+} \rightarrow Fe^{3+} + Fe^{5+}$)[1–9]. In the CD states at low temperature the Fe^{3+} and Fe^{5+} ions are ordered in a rock-salt manner, and magnetic moments of the Fe ions give complicated magnetic structures. In the charge disproportionated $CaFeO_3$, both ferromagnetic and antiferromagnetic interactions compete with each other[10], and as the result, a helical magnetic structure is stabilized below 115 K, which is below the CD transition temperature[11,12]. In the CD state of $CaCu_3Fe_4O_{12}$, on the other hand, a ferrimagnetic structure, where the *A*-site Cu spins couple antiferromagnetically with the *B*-site Fe spins, is stabilized[13]. Strong antiferromagnetic interactions between the *A*-site Cu^{2+} and *B*-site Fe^{3+} spins and between the Cu^{2+} and Fe^{5+} spins force to align the nearest neighbor Fe^{3+} and Fe^{5+} spins ferromagnetic.

We recently found that a similar CD occurred in the two-dimensional Fe^{4+} sublattice of the layered double perovskite Ca_2FeMnO_6, which consists of alternately stacked $Fe^{4+}O_6$ and MnO_6 octahedral layers[14,15]. In that material the Fe^{4+} in the two-dimensional layers shows CD below about 200 K, and the resultant Fe^{3+} and Fe^{5+} are ordered in a checkerboard manner. Further cooling results in a magnetic transition at 95 K, and an unusual noncollinear ferrimagnetic spin structure is stabilized. The neighboring spins in the FeO_6 octahedral layers, *i.e.* the charge disproportionated Fe^{3+} and Fe^{5+} spins, couple antiferromagnetically, resulting in ferrimagnetism[16].

In the examples described above, CD of the unusual high valence Fe^{4+} ions produces large $Fe^{3+}O_6$ and small $Fe^{5+}O_6$ octahedra alternately three-dimensionally ($CaFeO_3$ and $CaCu_3Fe_4O_{12}$) or two-dimensionally (Ca_2FeMnO_6). Thus, freezing of a $Fe^{4+}O_6$ breathing phonon mode appears to be responsible for causing such unusual charge behaviors. Additionally, in the CD states at low temperature, the nearest neighbor Fe^{3+} and Fe^{5+} spin pairs play important role in the magnetism, although the observed magnetic structures of the compounds are rather complicated due to the competing magnetic interactions. Considering the long-range charge and spin orders in the CD states, rigidly-arranged neighboring Fe^{4+} network seems to be important to cause the charge disproportionation behavior. Our primary concern is thus "to break the rigid Fe^{4+} network". For this purpose we have synthesized $CaFe_{0.5}Mn_{0.5}O_3$, which has a chemical composition identical to that of the layered double perovskite Ca_2FeMnO_6 but a disordered arrangement of *B*-site Fe and Mn. The compound contains Fe^{4+} randomly distributed at the half of the *B* sites, and thus stabilization of the long-range charge and spin orders of Fe^{3+} and Fe^{5+} is expected to be challenging. In the present study, we found, surprisingly, that this *B*-site-disordered $CaFe_{0.5}Mn_{0.5}O_3$ also

shows a CD of Fe^{4+} at a low temperature. We have used neutron powder diffraction (NPD) analysis to investigate the magnetic structure of this newly synthesized compound, and here we compare the crystal and magnetic structures of the *B*-site-disordered $CaFe_{0.5}Mn_{0.5}O_3$ with those of the layered *B*-site-ordered Ca_2FeMnO_6. We also discuss the CD and magnetic transition behaviors of this new phase.

Experiments

A polycrystalline sample of $CaFe_{0.5}Mn_{0.5}O_3$ was synthesized in a solid-state reaction under a high-pressure and high-temperature condition. A mixture of stoichiometric amounts of $CaCO_3$, Fe_2O_3, and $MnCO_3$ was calcined at 1250°C in air. The calcined powder was then sealed in a Pt capsule with the oxidizing agent $KClO_4$ and held at 5.3 GPa and 1100°C for 30 minutes before quenching to room temperature. The pressure was then reduced slowly to ambient and the reacted sample was removed from the capsule, washed several times with distilled water to remove residual KCl and $KClO_4$, and was then dried.

The crystal and magnetic structures were analyzed by measuring NPD patterns. Time-of-flight NPD experiments were performed at the WISH beamline of ISIS at RAL. The data were analyzed with the FullProf Rietveld program[17]. The valence state of Fe was estimated with Mössbauer spectroscopy measurements. The spectra were measured in transmission geometry with a constant-acceleration spectrometer using a $^{57}Co/Rh$ radiation source and were fitted with Lorentzian functions. Magnetic properties were measured with a commercial Quantum Design MPMS SQUID magnetometer.

Results and Discussion

Figure 1(a) shows the NPD pattern at room temperature and the result of crystal structure refinements for the obtained $CaFe_{0.5}Mn_{0.5}O_3$. The corresponding pattern and results for the layered double perovskite are shown in Fig. 1(c). In the pattern for $CaFe_{0.5}Mn_{0.5}O_3$ neither superstructure peaks related to the Fe/Mn ordering at the *B*-site (e.g. those at d =3.5 and 7.5 Å seen in the pattern for layered Ca_2FeMnO_6) nor diffuse intensities due to the short range orderings of the *B*-site cations are evident. The observed diffraction pattern of $CaFe_{0.5}Mn_{0.5}O_3$ is well reproduced with a $GdFeO_3$-type perovskite structure model with a space group *Pnma* and a $\sqrt{2}a\times 2a\times\sqrt{2}a$ unit cell (a represents the lattice constant of the simple perovskite structure, ~3.8 Å), and the refinement results are listed in Table 1. The Fe and Mn ions occupy the 4*b* site, and the refined occupancies are 51.2(2)/48.8 % for Fe/Mn. Note also that each refined lattice parameter is, in keeping with Vegard's law, between the parameters corresponding to the two end-composition compounds of $CaFeO_3$ and $CaMnO_3$[8,18–20]. The above results confirm the random distribution of the Fe and Mn ions at the *B* site in $CaFe_{0.5}Mn_{0.5}O_3$.

The valence state of Fe in $CaFe_{0.5}Mn_{0.5}O_3$ was verified from the ^{57}Fe Mössbauer spectra. As shown in Fig. 2 (a), the observed spectrum at room temperature is well fitted with a single paramagnetic component with the isomer shift (*IS*) of 0.04 mms^{-1}. This small value is typical for unusual Fe^{4+} and is also very close to that observed in the layered $Ca_2Fe^{4+}MnO_6$ (0.02 mms^{-1}). The absence of any trace of Fe^{3+} in the spectrum confirms that all the Fe ions in the $CaFe_{0.5}Mn_{0.5}O_3$ were Fe^{4+}. Therefore, two samples having an identical chemical composition with the unusually high valence Fe^{4+} at room temperature can be made: one is the present *B*-site-disordered $CaFe_{0.5}Mn_{0.5}O_3$ and the other is the layered *B*-site-ordered Ca_2FeMnO_6 reported in Refs (14-15). Comparing the Mössbauer spectra, one sees that the local environments of Fe^{4+} in the two samples appear to be quite similar to each other in spite of the difference in the degree of long range order.

Importantly, as shown in the Mössbauer spectra at 3 K [Fig. 2(b)], Fe^{4+} in the *B*-site-disordered $CaFe_{0.5}Mn_{0.5}O_3$ shows CD at low temperatures. The observed spectrum is reproduced with two magnetically ordered sextets with almost equal intensities. Their *IS*s are –0.01 and 0.35 mms^{-1} and the corresponding hyperfine fields (*HF*) are 28.8 and 44.3 T, which are close to the values for charge-disproportionated Fe^{5+} (*IS* = –0.01 mms^{-1} and *HF* = 27.4 T) and Fe^{3+} (*IS* = 0.35 mms^{-1} and *HF* = 43.4 T) in the layered *B*-site-ordered Ca_2FeMnO_6. It is surprising that all the Fe^{4+} ions randomly distributed at the half of the *B* sites also show CD. CD of Fe^{4+} has been reported to occur in the three-dimensional cubic ($CaFeO_3$ and $CaCu_3Fe_4O_{12}$) and two-dimensional square (Ca_2FeMnO_6) sublattices of Fe^{4+}, producing respectively the rock-salt-type and checkerboard-type orderings of Fe^{3+} and Fe^{5+} (Ref. 12). The present results, however, show that a complete three or two dimensional network of the unusually high valence Fe^{4+} ions is not necessary for the CD transition. The result also implies that the CD transition is induced by the electronically instability, not by the instabilities of phonons.

It is difficult to determine the distribution of Fe^{3+} and Fe^{5+} in the CD state from the diffraction data. In the NPD pattern at 2K shown in Fig. 1(b), neither apparent superstructure nor distortion from the room temperature crystal structure is detected, and the nuclear diffraction intensities are essentially the same as those at 300 K. Although the CD transition is often accompanied by a crystal structure transition, this appears to be suppressed by substitution with Mn^{4+} in the present *B*-site-disordered $CaFe_{0.5}Mn_{0.5}O_3$. This also causes difficulty in determining the CD transition temperature form the structural change.

The magnetic properties and structure of charge-disproportionated $CaFe_{0.5}Mn_{0.5}O_3$ are of particular interest. As shown by the temperature dependence of magnetic susceptibility [Fig. 3(a)], $CaFe_{0.5}Mn_{0.5}O_3$ shows a magnetic transition around 90 K. Note, it is not clear at the current stage whether the magnetic transition occurs below the CD transition as seen in the layered double perovskite Ca_2FeMnO_6, because the CD transition temperature in the present

compound has not been determined from the structural changes. However, the experimental results, that Mössbauer spectrum under the magnetic transition temperature consists of the two components and that the magnetic susceptibility shows no anomalies below the magnetic transition temperature, strongly suggest that at least the magnetic transition occurs in the CD state. Therefore, the magnetic transition temperature of $CaFe_{0.5}Mn_{0.5}O_3$ is the same as or lower than the CD transition temperature. The 90-K magnetic transition temperature is very close to the magnetic transition temperature of the layered double perovskite Ca_2FeMnO_6 [14-16]. Field dependence of the magnetization revealed that the compound has a small spontaneous magnetization of about 0.2 μ_B per $CaFe_{0.5}Mn_{0.5}O_3$, which is also very close to that of the layered and ordered Ca_2FeMnO_6 [Fig. 3(b)]. Local magnetic environments of the charge-disproportionated Fe^{3+} and Fe^{5+} evaluated from the *HF* values in the Mössbauer spectrum [Fig. 2(b)] are also not so different from those in the layered *B*-site-ordered compound. It is thus notable that the two compounds with different *B*-site cation ordered structures show similar magnetic behaviors.

In contrast, magnetic reflections of $CaFe_{0.5}Mn_{0.5}O_3$ in the NPD pattern obtained at 2 K [Fig. 1(b)] are very different from those of the layered *B*-site-ordered Ca_2FeMnO_6, indicating that the magnetic structures of the two compounds are not identical. The present $CaFe_{0.5}Mn_{0.5}O_3$ shows an apparent magnetic superstructure peak at $d \approx 4.3$ Å, while the layered *B*-site-ordered Ca_2FeMnO_6 shows three strong magnetic superstructure peaks indexed as 010/001, 110/011, and 210/201 [Fig. 1(d)]. The peak at $d \approx 4.3$ Å corresponds to 110 or 011 reflections of a $\sqrt{2}a \times 2a \times \sqrt{2}a$ unit cell, indicating the presence of a G-type antiferromagnetic (AFM) spin structure, where all the nearest neighboring spins couple antiparallel to each other. The fit of a G-type AFM spin structure to the NPD data at 2 K gives an average refined moment of 0.58 μ_B per cation. This ordered moment is very small compared to the ideal 3.5 μ_B average magnetic moment for 25% Fe^{3+} (S = 5/2), 25% Fe^{5+} (S = 3/2), and 50% Mn^{4+} (S = 3/2) ions randomly distributed at the *B* sites and demonstrates that there is large disordered component to the magnetic order. It is important to point out that the present *B*-site disordered $CaFe_{0.5}Mn_{0.5}O_3$ shows higher structural symmetry due to randomly distributed Fe and Mn ions than the layer-ordered Ca_2FeMnO_6. Because the collinear G-type AFM structure is much simpler than the noncollinear magnetic structure observed in the layer-ordered Ca_2FeMnO_6, the difference in the magnetic structures between the two compounds appears to be reasonable in symmetrical stability point of view.

This simple G-type AFM spin structure indicated by the NPD result is apparently incompatible with the spontaneous magnetization of 0.2 μ_B observed in the magnetization measurement. There are two plausible explanations for this. The first is that weak ferromagnetism is symmetry-allowed in *Pnma* perovskites with G-type AFM order, and is

observed in many RFeO$_3$ and RCrO$_3$ materials for various rare earth elements R[21-23]. A second explanation is that ferrimagnetism arise from the formation of charge disproportionated Fe^{3+} and Fe^{5+} ordering. This is the more likely origin given the similarity of the magnetic properties to those of the cation and charge ordered Ca_2FeMnO_6. Local charge ordering below the CD transition temperature favors Fe^{3+}-O-Fe^{5+} arrangements over the Fe^{3+}-O-Fe^{3+} and Fe^{5+}-O-Fe^{5+} alternatives, so in the G-type AFM spin structure below the magnetic transition temperature, which is also below the CD transition temperature, the Fe^{3+} magnetic moments are aligned in the opposite direction to the Fe^{5+} moments, giving net ferrimagnetic moments (Fig. 4). The Mn^{4+} cations are equally substituted for Fe^{3+} and Fe^{5+}, and so their ordered magnetic moments cancel each other, and so do not give net magnetization. This model predicts an ideal magnetization of 0.5 μ_B for $CaFe_{0.5}Mn_{0.5}O_3$, which is consistent with the observed magnetization of 0.2 μ_B given further reductions due to disorder. Although this model assumes dominant AFM Fe^{3+}-O-Fe^{5+} interactions, the observed helical magnetic structure of $CaFeO_3$ shows that these connections can lead to competing AFM and ferromagnetic (FM) interactions. Competition between AFM and FM Fe^{3+}-O-Fe^{5+} and also Mn^{4+}-O-Fe^{5+} interactions, plus the structural disorder present in $CaFe_{0.5}Mn_{0.5}O_3$ results in a large proportion of the spins being disordered or remaining dynamic below the magnetic ordering transition. This is consistent with the 5 K paramagnetic susceptibility of $CaFe_{0.5}Mn_{0.5}O_3$ being greater than that of *B*-site cation-ordered Ca_2FeMnO_6, as shown by the high field *M*-*H* slopes in Fig. 3(b).

It is worth noting again that the Fe^{3+} and Fe^{5+} Mössbauer spectra and the magnetic behaviors of the present $CaFe_{0.5}Mn_{0.5}O_3$ are quite similar to those of the layered *B*-site-ordered Ca_2FeMnO_6 with the same chemical composition but a different magnetic structure. Although the local aliovalent Fe^{3+}-O-Fe^{5+} arrangements in the CD states play an important role in determining the magnetic structures in both compounds, the *B*-site ordering makes the magnetic structures different.

Conclusions

The *B*-site-disordered perovskite-structure oxide $CaFe_{0.5}Mn_{0.5}O_3$ was obtained using high-pressure synthesis. The NPD structure analysis and the Mössbauer spectroscopy results revealed that the compound contains Mn^{4+} and unusually high valence Fe^{4+} ions randomly distributed over the *B* sites, and that the chemical composition of this oxide is identical to that of the layered *B*-site-ordered Ca_2FeMnO_6. Like Ca_2FeMnO_6, $CaFe_{0.5}Mn_{0.5}O_3$ shows CD of Fe^{4+} at low temperatures and shows magnetic transition at 90 K. The CD in the *B*-site disordered $CaFe_{0.5}Mn_{0.5}O_3$ suggests that freezing of breathing mode phonon is not necessary for the transition. Magnetic structure analysis with the NPD data revealed that $CaFe_{0.5}Mn_{0.5}O_3$ has a G-type AFM spin structure although a small spontaneous magnetization is observed in

magnetization measurements. This is consistent with local charge ordering that gives rise to Fe^{3+}-O-Fe^{5+} antiferromagnetic interactions so inexact cancellation of opposing Fe^{3+} and Fe^{5+} spins produces ferrimagnetism. The magnetic structure of $CaFe_{0.5}Mn_{0.5}O_3$ is thus very different from the noncollinear magnetic structure of Ca_2FeMnO_6.

Acknowledgements

We thank P. Manuel and D. Khalyavin for their help with NPD experiments at ISIS, Rutherford Appleton Laboratory, UK. The synchrotron radiation experiments at SPring-8 were performed with the approval of the Japan Synchrotron Radiation Research Institute (proposal Nos: 2015B1718). This work was supported by Grants-in-Aid for Scientific Research (Nos. 22740227, 24540346, 16H00888, and 16H02266), by JSPS Core-to-Core program, by a grant for the Joint Project of Chemical Synthesis Core Research Institutions from MEXT, and by a JST-CREST program of Japan. Support was also provided by EPSRC, STFC and the Royal Society, UK.

References

[1] M. Takano, N. Nakanishi, Y. Takeda, S. Naka, and T. Takada, Mater. Res. Bull. **12**, 923 (1977).

[2] M. Takano, N. Nakanishi, Y. Takeda, and S. Naka, Le Journal de Physique Colloques **40**, C2 (1979).

[3] I. Yamada, K. Takata, N. Hayashi, S. Shinohara, M. Azuma, S. Mori, S. Muranaka, Y. Shimakawa, and M. Takano, Angew. Chem. **120**, 7140 (2008).

[4] Y. Shimakawa and M. Takano, Z. Anorg. Allg. Chem. **635**, 1882 (2009).

[5] J. Zaanen, G.A. Sawatzky, and J.W. Allen, Phys. Rev. Lett. **55**, 418 (1985).

[6] A.E. Bocquet, A. Fujimori, T. Mizokawa, T. Saitoh, H. Namatame, S. Suga, N. Kimizuka, Y. Takeda, and M. Takano, Phys. Rev. B **45**, 1561 (1992).

[7] S. Kawasaki, M. Takano, R. Kanno, T. Takeda, and A. Fujimori, J. Phys. Soc. Jpn. **67**, 1529 (1998).

[8] T. Takeda, R. Kanno, Y. Kawamoto, M. Takano, S. Kawasaki, T. Kamiyama, and F. Izumi, Solid State Sci. **2**, 673 (2000).

[9] W.-T. Chen, T. Saito, N. Hayashi, M. Takano, and Y. Shimakawa, Sci. Rep. **2**, 449 (2012).

[10] M. Mostovoy, Phys. Rev. Lett. **94**, 137205 (2005).

[11] S. Morimoto, T. Yamanaka, and M. Tanaka, Phys. B **237**–**238**, 66 (1997).

[12] P.M. Woodward, D.E. Cox, E. Moshopoulou, A.W. Sleight, and S. Morimoto, Phys. Rev. B **62**, 844 (2000).

[13] M. Mizumaki, W.T. Chen, T. Saito, I. Yamada, J.P. Attfield, and Y. Shimakawa, Phys. Rev. B **84**, 094418 (2011).

[14] S. Ganesanpotti, C. Tassel, N. Hayashi, Y. Goto, G. Bouilly, T. Yajima, Y. Kobayashi, and H. Kageyama, Eur. J. Inorg. Chem. **2014**, 2576 (2014).

[15] Y. Hosaka, N. Ichikawa, T. Saito, M. Haruta, K. Kimoto, H. Kurata, and Y. Shimakawa, Bull. Chem. Soc. Jpn. **88**, 657 (2015).

[16] Y. Hosaka, N. Ichikawa, T. Saito, P. Manuel, D. Khalyavin, J.P. Attfield, and Y. Shimakawa, J. Am. Chem. Soc. **137**, 7468 (2015).

[17] J. Rodríguez-Carvajal, Phys. B **192**, 55 (1993).

[18] Y. Takeda, S. Naka, M. Takano, T. Shinjo, T. Takada, and M. Shimada, Mater. Res. Bull. **13**, 61 (1978).

[19] K.R. Poeppelmeier, M.E. Leonowicz, J.C. Scanlon, J.M. Longo, and W.B. Yelon, J. Solid State Chem. **45**, 71 (1982).

[20] Y. Nakahara, S. Kato, M. Sugai, Y. Ohshima, and K. Makino, Mater. Lett. **30**, 163 (1997).

[21] Y.B. Bazaliy, L.T. Tsymbal, G.N. Kakazei, V.I. Kamenev, and P.E. Wigen, Phys. Rev. B **72**, 174403 (2005).

[22] S. Yuan, Y. Wang, M. Shao, F. Chang, B. Kang, Y. Isikawa, and S. Cao, J. Appl. Phys. **109**,

07E141 (2011).

[23] B. Rajeswaran, D.I. Khomskii, A.K. Zvezdin, C.N.R. Rao, and A. Sundaresan, Phys. Rev. B **86**, 214409 (2012).

Table 1. Refined crystal structure parameters of $CaFe_{0.5}Mn_{0.5}O_3$ at room temperature (obtained in Rietveld analysis of the NPD data.) Space group, *Pnma*, a = 5.3177(3) Å, b = 7.5035(4) Å, and c = 5.3041(3) Å. Rwp = 4.59%.

Atom	x	Y	Z	B (Å^2)	occupancy
Ca	0.0282(6)	0.25	0.993(1)	0.94(6)	1.0
Fe	0.0	0.0	0.5	0.11(7)	0.510(2)
Mn	0.0	0.0	0.5	0.11(7)	0.490(2)
O1	0.2892(5)	0.0350(4)	0.7153(6)	1.26(6)	1.0
O2	0.4879(6)	0.25	0.0617(7)	0.70(7)	1.0

Figure captions

Figure 1. Neutron powder diffraction patterns and refinement results for *B*-site-disordered perovskite $CaFe_{0.5}Mn_{0.5}O_3$ (a) at 300 and (b) 2 K. Corresponding patterns and results for the layered double perovskite Ca_2FeMnO_6 at 300 (c) and (d) 2 K are reproduced from (Ref. 14). The dots, black lines, blue lines, and vertical marks represent observed patterns, calculated patterns, differences between observed and calculated intensities, and Bragg refraction points, respectively. Marked peaks are typical magnetic reflections.

Figure 2. Mössbauer spectra of *B*-site-disordered $CaFe_{0.5}Mn_{0.5}O_3$ measured (a) at room temperature and (b) 3 K. The circles are observed data, and the spectra are fitted with (a) a singlet component and (b) two sextets corresponding to Fe^{3+} and Fe^{5+} components.

Figure 3. Magnetic properties of *B*-site-disordered $CaFe_{0.5}Mn_{0.5}O_3$ (red) together with those of the layered *B*-site-ordered double perovskite Ca_2FeMnO_6 (blue). (a) Temperature dependence of magnetic susceptibility χ. (b) Magnetic field dependence of magnetic moment.

Figure 4. Idealized model for the spin and charge ordering in *B*-site-disordered $CaFe_{0.5}Mn_{0.5}O_3$. Red, blue, and white arrows represent magnetic spins of Fe^{3+}, Fe^{5+}, and Mn^{4+}, respectively. G-type antiferromagnetism over local Fe^{3+}-O-Fe^{5+} arrangements give rise to the observed ferrimagnetism.

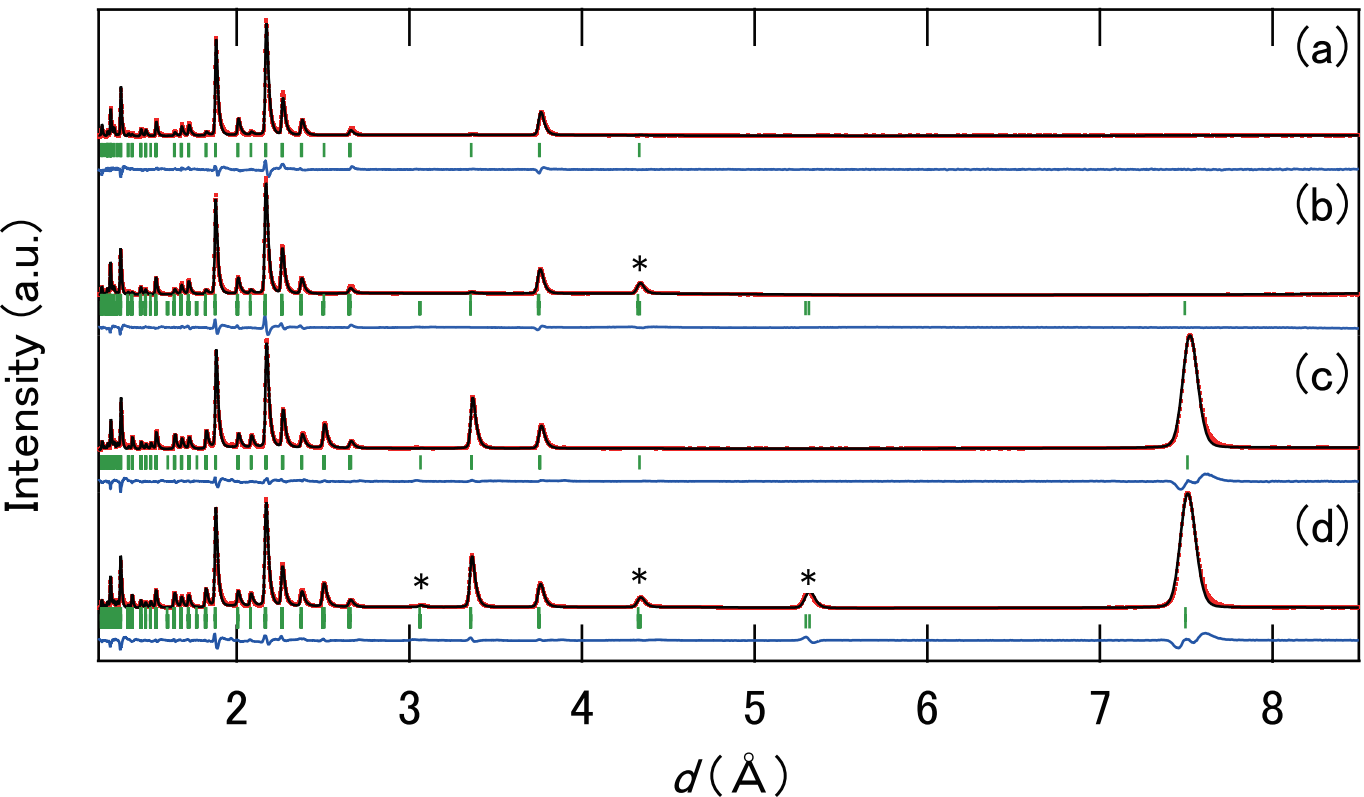
(a)
(b)
(c)
(d)
*
*
*
*
Intensity (a.u.)
2
3
4
5
6
7
8
d (Å)

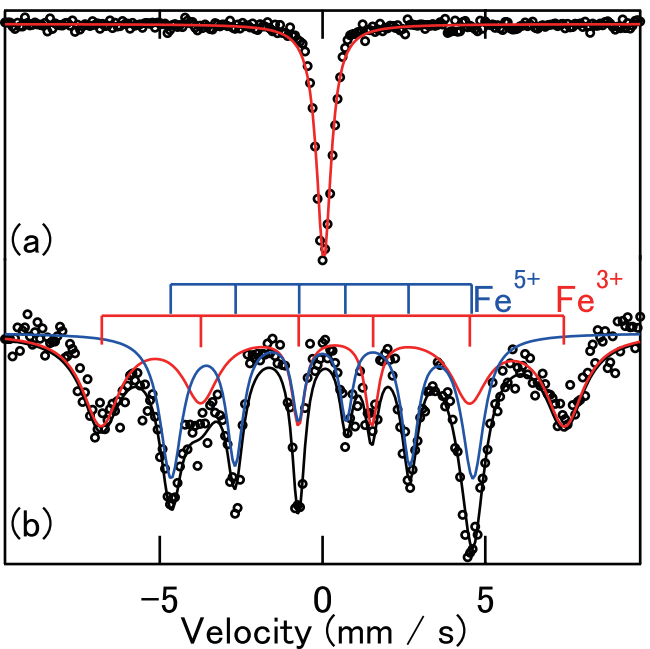
(a)
Fe5+
Fe3+
(b)
−5
0
5
Velocity (mm / s)

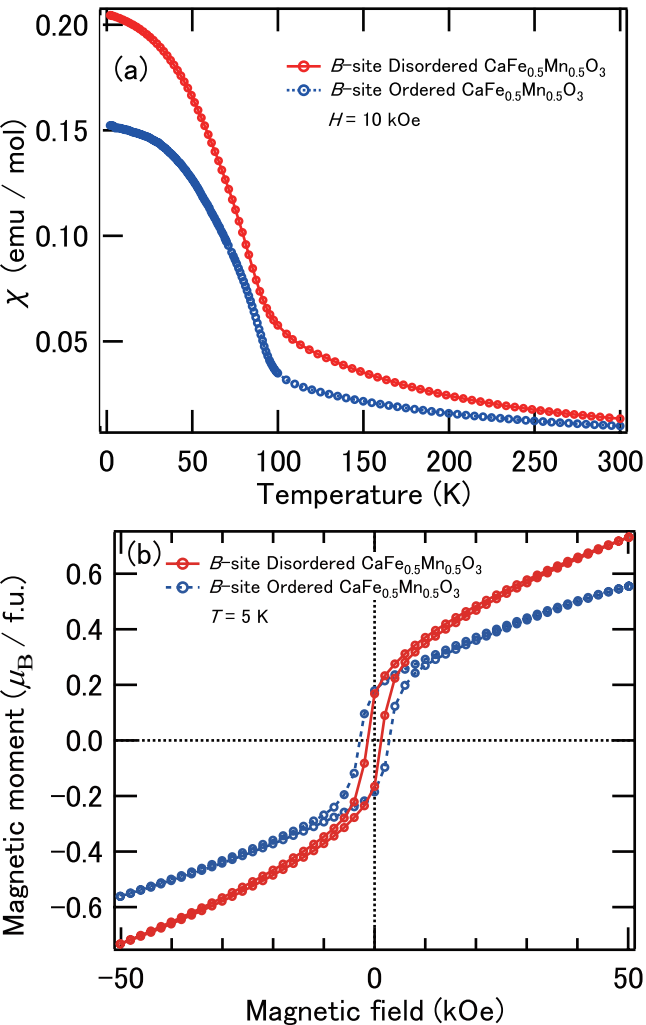
(a)
B-site Disordered CaFe0.5Mn0.5O3
B-site Ordered CaFe0.5Mn0.5O3
H = 10 kOe
χ (emu / mol)
0.20
0.15
0.10
0.05
0
50
100
150
200
250
300
Temperature (K)
(b)
B-site Disordered CaFe0.5Mn0.5O3
B-site Ordered CaFe0.5Mn0.5O3
T = 5 K
Magnetic moment (μB / f.u.)
0.6
0.4
0.2
0.0
−0.2
−0.4
−0.6
−50
0
50
Magnetic field (kOe)

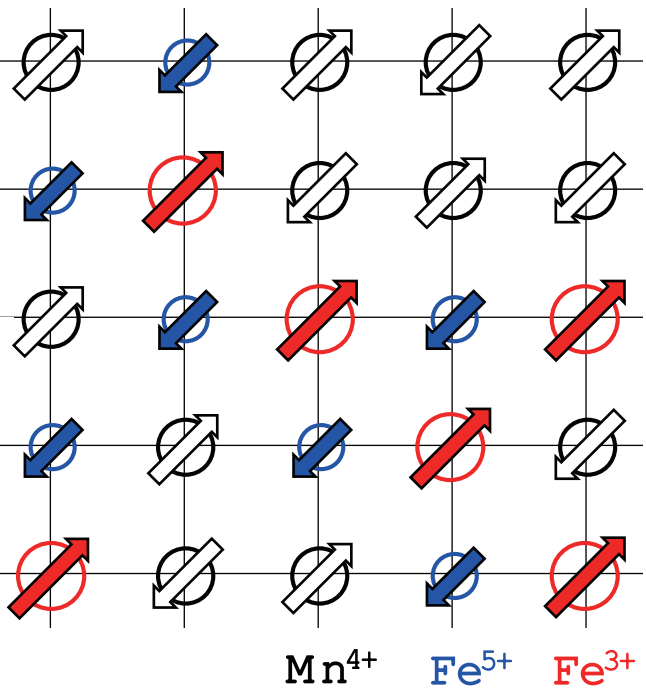
Mn^{4+}
Fe^{5+}
Fe^{3+}